ENVIRONMENTAL RESEARCH 49, 295–317 (1989)

X-Ray Fluorescence: Issues Surrounding the Application of a New Tool for Measuring Burden of Lead

HOWARD HU,* FREDRIC L. MILDER,† AND DOUGLAS E. BURGER†

Channing Laboratory, Harvard Medical School, and Department of Epidemiology, Harvard School of Public Health, Boston, Massachusetts 02115, and †ABIOMED, Inc., Danvers, Massachusetts 01923

Received August 26, 1988

Studies of lead toxicity would greatly benefit from a convenient, noninvasive measure of body lead burden. X-ray fluorescence (XRF) promises to provide such a measure by rapidly estimating lead content in bone, the repository of greater than 95% of an adult's lead stores (73% in children). Two separate XRF techniques exist, L-XRF and K-XRF. They differ in terms of calibration method and type of bone sampled. They also involve different radiation energies; however, radiation doses and concomitant risks are similarly low. Since interpretation of an XRF measurement depends to an extent on the distribution of lead in the skeleton, this topic is reviewed. Available data suggest that trabecular and cortical bone comprise two distinct compartments with regard to lead kinetics. Within each compartment, however, there also appears to be a significant degree of variability. Furthermore, there is evidence to suggest that the subperiosteal surface layer of cortical bone has a pattern of lead absorption and release that is different from the rest of cortical bone. This may have implications for (1) the choice of XRF technique, since the L-XRF technique measures lead in surface bone, whereas the K-XRF technique derives an estimate of lead from the full thickness of bone, and (2) the selection of bone sites for taking XRF measurements. More research is necessary to fully optimize the applicability of the XRF instrument.

INTRODUCTION

Current Methods of Estimating Body Lead Burden

Lead is a familiar topic in environmental science. Clinical studies of lead's effect on health have traditionally relied on blood lead levels as an indicator of lead exposure. As research continues, however, investigators are beginning to question whether blood lead level provides adequate information.

While blood lead level, which has a half-life of 2 to 3 weeks (Heard and Chamberlain, 1984), mostly reflects recent environmental lead exposure, some manifestations of lead toxicity seem to correlate best with measures of cumulative body lead burden. For instance, in studies of lead nephropathy, body burden of lead as measured by the EDTA mobilization test has a better correlation than blood lead level with renal dysfunction (Crasswell *et al.*, 1984; Batuman *et al.*, 1981, 1983; Wedeen *et al.*, 1986). Increased lead burden as measured by tooth lead, rather than blood lead levels, has been found to have an association with diminished neuropsychological performance in children (Needleman, 1982; Marecek *et al.*, 1983; Winneke *et al.*, 1983). EDTA lead burden has also been related to abnormal somatosensory evoked potentials in lead-exposed workers (Araki, 1986).

Clearly, future studies on the effects of lead would greatly benefit from the

0013-9351/89 $3.00

inclusion of an exposure parameter that reflected lead burden. Currently available techniques for measuring lead burden, however, suffer from several weaknesses.

Chelating agents, such as $CaNa_2EDTA$ and penicillamine, have been widely used to mobilize stored lead into plasma. Lead so mobilized is filtered into urine, where it can be measured. The quantity of chelated lead in response to a standard dose of chelating agent is in proportion to the cumulative lead burden. A number of studies on small groups of subjects using chelation tests have uncovered elevated lead burdens in subjects with possible lead-induced end organ damage (Batuman *et al.*, 1981, 1983; Craswell *et al.*, 1984; Wedeen *et al.*, 1986; Pinto de Almeida *et al.*, 1987).

The degree to which lead stores in different organs contribute to lead measurements is unclear, however. In animal studies, Hammond and colleagues report that $CaNa_2EDTA$ mainly releases bone deposits of lead, although there is also some release of soft tissue lead stores as well (Hammond *et al.*, 1967; Hammond, 1971). On the other hand, Castellino and Aloj report that $CaNa_2EDTA$ mobilizes lead primarily from soft tissues such as liver, kidney, lung, spleen, and heart, and not from bone (Castellino and Aloj, 1965). Several human studies report a wide discrepancy between results of the $CaNa_2EDTA$ mobilization test and bone lead content (Germain *et al.*, 1984; Westerman *et al.*, 1965).

Some authors point out that although mobilization tests may not accurately reflect total body lead burden in an absolute sense, studies linking mobilizable lead with chronic toxicity suggest that mobilizable lead reflects a biologically active fraction of the total burden (Nordberg, 1976; Araki and Ushio, 1982; Chisholm *et al.*, 1975).

A practical disadvantage of mobilization tests, however, is that they require the accurate collection of urine for hours or days. This is unrealistic for large population studies. Moreover, $CaNa_2EDTA$, the most widely used agent, requires injection or iv infusion. Although penicillamine is an oral agent, it is less potent than $CaNa_2EDTA$ and gives a smaller "chemical biopsy" of lead (Harris, 1958; Westerman *et al.*, 1965).

Tooth levels of lead, as mentioned above, have been used as indicators of lead burden in research on children. Such studies, however, rely on the analysis of lead in shed teeth. This has obvious practical limitations with regard to doing research. The kinetics of lead in teeth also seems to be distinct from that of the skeleton, where most of the lead burden resides (Steenhout, 1982; Holtzman *et al.*, 1970).

Other biochemical markers of lead toxicity, such as δ-aminolevulinic dehydratase (ALAD), urinary δ-aminolevulinic acid, and erythrocyte protoporphyrin, have been shown to be sensitive to lead burden. As biochemical intermediates in hemoglobin synthesis, however, these parameters are sensitive to other confounding perturbations besides lead. Little evidence exists to suggest that they can be used to quantitatively estimate cumulative body lead burden.

X-Ray Fluorescence

Recently, attention has been given to X-ray fluorescence (XRF), a method that uses low-dose radiation to estimate rapidly lead content in the bone being measured. Field studies of XRF have already demonstrated that the method is trans-

portable, convenient for patients, and measures bone lead content fairly accurately in comparison to measurements made by atomic absorption spectrometry. XRF measurements have also been shown to correlate well with body lead burden as estimated by EDTA chelation (Wedeen *et al.*, 1987) and time-integrated blood lead indices (Somervaille *et al.*, 1988).

A constant 90–95% of total body lead burden in adults (73% in children) is contained in bone (Barry and Mossman, 1970; Schroeder and Tipton, 1968). Thus, an XRF estimate of skeletal lead burden theoretically should serve as a reasonable proxy for total body lead burden. In addition, bone lead is more mobile than it was often previously assumed to be (U.S. EPA, 1986). Kinetic modeling has shown that this fraction can be naturally resorbed into blood (Rabinowitz, 1976). Several reports have also suggested that mobilization of bone lead stores by malnutrition, pregnancy, chemotherapy, and metabolic bone disease states can lead directly to toxicity (Barker *et al.*, 1982; Thompson and Robertson, 1985; El-Sharkawi *et al.*, 1986; Brown and Tompsett, 1945). Physiologic states such as pregnancy (Zaric *et al.*, 1987), lactation (Manton, 1985), and postmenopausal osteoporosis (Silbergeld *et al.*, 1988) have been shown in population studies to heighten release of bone stores of lead into blood.

There has been little formal discussion of how to apply the XRF tool, however. In this paper, we shall summarize recent developments in the XRF technique with regard to capabilities and limitations; the state of knowledge regarding lead distribution in bone; and issues that need to be addressed in order to optimize its use for measuring lead burden in research and clinical practice.

XRF: The Technique

The use of XRF as a method of *in vivo* bone lead quantification has been under development for 12 years (Ahlgren *et al.*, 1976). For in-depth discussions of technical issues pertaining to the physics of measuring lead in bone with XRF, the reader is referred elsewhere (Laird *et al.*, 1982; Scott and Chettle, 1986; Wielopolski *et al.*, 1983; Jones *et al.*, 1987).

As understanding of lead kinetics in bone and experience with the XRF technique have grown, researchers have begun to narrow their variations in technique. What remains are two basic approaches, K-XRF and L-XRF. The underlying principles of each are similar, as shown in Figs. 1 and 2.

XRF is an atomic radiation that may be pictured by considering an atom as consisting of electrons existing in layers or shells having a regular progression in the number of electrons as one passes from element to element. It is customary to give letter designations to the sets of electrons within the same principal shell. Thus, electrons of the innermost shell ($n = 1$) are called K electrons, the second shell ($n = 2$), L electrons, the third shell ($n = 3$), M electrons, and so forth. Most of the properties of atoms such as electrical, chemical, optical, etc., that we experience on a daily basis depend upon the configurations of the *outer*most electrons. Only in the event of a very energetic disturbance are the tightly bound *inner* electrons involved. For example, for a lead (Pb) atom ($z = 82$), only 7.4 eV of energy is required to remove an outermost electron, but 10,500 eV (10.5 keV)

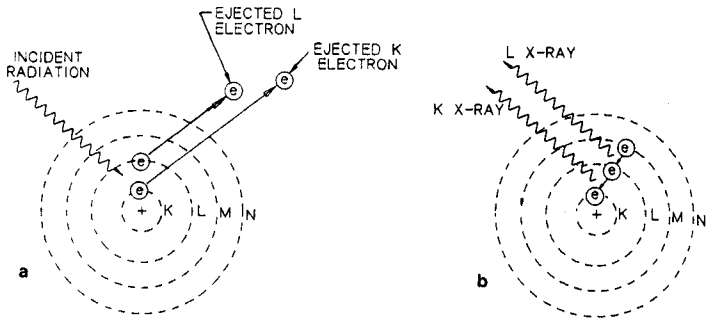

FIG. 1. X-ray fluorescence (a) high energy radiation is incident on an atom; it penetrates to one of the two innermost shells and ejects either a K- or L-shell electron depending on the incident energy (b) One of the bound L or M electrons then makes a transition, filling the vacancy left in the K or L shell and emitting a K- or L-fluorescent X-ray in the process.

to remove an L-shell electron, and an energy of 88,000 eV (88 keV) is necessary to remove one of the K-shell electrons (Richtmyer *et al.*, 1969).

In Fig. 1 is illustrated a schematic representation of the production of fluorescent X-rays. In Fig. 1a, high-energy radiation is incident on an atom where it penetrates to the innermost shell(s), ejecting either an L- or K-shell electron depending on the incident energy. Next, one of the L- or M-shell electrons makes a transition, filling the vacancy left by the ejected electron and emitting either a K- or L-fluorescent X-ray in the process. This emitted energy is characteristic of the element which absorbed the original X-ray.

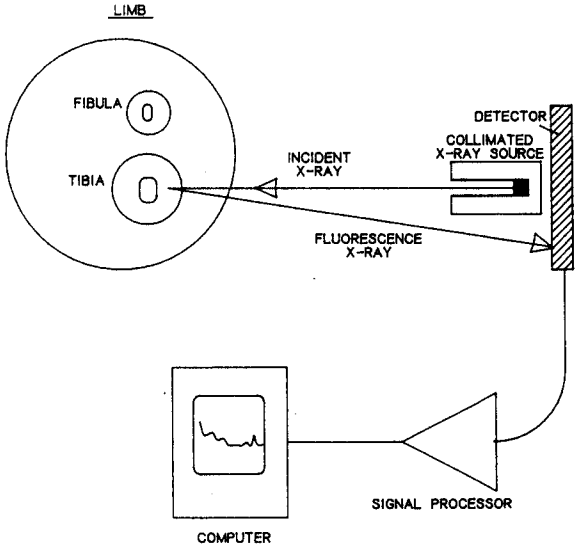

FIG. 2. Diagram indicating a fluorescence detection system used in making X-ray fluorescence measurements. The target, in this instance the tibia, is illuminated by a collimated X-ray source. The resulting Pb fluorescence X-rays are detected and preprocessed before routing to a computer for display and further processing.

Figure 2 is a block diagram of an XRF detection system in which a collimated X-ray source is exposing a leg limb. The resulting signal sensed by the detector undergoes processing to prepare it for presentation to the computer for subsequent display and analysis. A detection system which collects, counts, and analyzes the emitted X-rays according to their energy is therefore able to determine how much of each element is present in the sample.

In L-XRF, the incident X-ray beam is derived from either a radioisotope source or an X-ray generator, and L-X-rays are produced at relatively low energies. A ^{109}Cd source has been used in several studies to induce L-X-rays at energies of 10.549 and 12.611 keV (Wielopolski *et al.*, 1981, 1983, 1986). L-XRF has also been studied using an ^{125}I radioisotope (Wielopolski *et al.*, 1983). Recent work has focused on the use of a low-energy X-ray generator and polarizer to induce the L-X-rays. At these low energies, calibration of the measurement to units of lead concentration must take into account attenuation of the signal by overlying skin. This is done by measuring the skin thickness overlying the target tibia using an ultrasound transducer and applying an attenuation correction. Calibration of the adjusted signal is made by plotting the signal against a series of L-XRF measurements taken on cadaver legs with known bone lead concentrations.

In K-XRF, the incident X-ray beam is derived from a radioisotope source. The choice of isotope has varied from ^{57}Co (Ahlgren *et al.*, 1976, 1980; Price *et al.*, 1984), with excitation γ-rays at energies of 122 and 136 keV, to, more recently, ^{109}Cd isotope (Somervaille *et al.*, 1985; Jones *et al.*, 1987), with an exciting γ-ray at 88 keV. ^{153}Gd has also been considered (Somervaille *et al.*, 1985), having an exciting γ energy at 97 keV. ^{109}Cd is presently used because it generates the greatest number of fluorescence X-rays per incident X-ray, thereby minimizing patient dose (Somervaille *et al.*, 1985; Wedeen *et al.*, 1987). Sensitivity can be increased at the expense of patient exposure, which varies approximately as the inverse of the square root of the dose. Calibration of the measurement to units of Pb (lead) concentration is done by counting, simultaneously with the Pb signal, the coherently scattered γ-rays to estimate Ca (calcium) content, and then multiplying the Pb/Ca ratio by a constant. In effect, this gives an estimate of Pb/bone mineral and has been shown to correlate well with Pb/bone ash weight (Somervaille *et al.*, 1986). The constant is determined empirically by relating the Pb/Ca ratio to bone lead concentrations determined by atomic absorption in a series of cadaver legs and phantoms.

Since radiation hazard is decreased by over an order of magnitude by using the appendicular skeleton, researchers using XRF instruments have focused their efforts on extremity bones such as the phalanges (Ahlgren *et al.*, 1980) and tibia. XRF measurements in the phalanges, however, have proved to be relatively insensitive, possibly due to the small volume of bone being measured, the unpredictable trabecular/cortical bone ratio (see below), and susceptibility of these bones to erosion and cyst formation in renal failure patients (Craswell *et al.*, 1986). Thus, researchers using both K-XRF and L-XRF have begun to focus primarily on the tibial midshaft as the sampling site.

Limit of Detection and Accuracy

Although there are several nuances in the mathematical definitions that have

been used by authors to describe limit of detection (Mattsson *et al.*, 1987), it can be generally defined as when the lead peak is three times the standard deviation on the underlying background. In both L-XRF and K-XRF, the rather poor signal-to-noise ratio has been a major obstacle to lowering the limit of detection of the instrument. In the L-XRF approach, the most recent advance has been to use a polarized beam and a 90° detection angle to reduce the background scatter (the noise under the signal). In the K-XRF, using a 180° detection angle without polarization has proved adequate.

Studies comparing XRF with atomic absorption spectroscopy (AAS) measurements of amputation and cadaver leg specimens have provided limited data on the accuracy and limit of detection of the two techniques. Direct comparisons of L-XRF in intact (undissected) leg specimens to AAS of the subsequently dissected bone have been made in two studies in which a combined total of 16 leg specimens were examined (Wielopolski *et al.*, 1983; Wielopolski *et al.*, in press). Correlation coefficients of $r = 0.90$ and $r = 0.95$ were obtained after applying an estimated correction factor for overlying skin thickness. Using background count data, minimum detection limits were calculated to be 22 ppm in the earlier study and 6.4 ppm in the latest study. No bone samples were examined that actually had AAS-measured bone lead concentrations below 12 μg/g wet wt.

Direct comparisons of K-XRF in intact leg specimens to AAS were made in one study of 6 leg specimens (Wedeen *et al.*, 1987). A correlation coefficient of $r = 0.98$ was found. A minimum detection limit was not calculated, but the authors noted that the technique measured a lead concentration of 10 μg/g wet wt with an error of 16%. Somervaille *et al.* compared XRF of dissected leg bones and AAS in a study including 30 tibia specimens ranging in lead concentration from approximately 4 to 40 μg/g wet bone (10.0 to 79.2 μg/g bone ash as measured by AAS) (Somervaille *et al.*, 1986). Since K-X-rays experience little of the attenuation that L-X-rays experience, these *in vitro* comparisons were assumed to have validity that would be similar to the *in vivo* situation. Using a paired *t* test, the authors found a low probability of a significant difference between the two measurement techniques. Using their published raw data, a correlation coefficient of 0.93 can be calculated. Somervaille *et al.* have estimated the minimum detection limit to be approximately 10 μg/g wet bone (Somervaille *et al.*, 1988). K-XRF researchers claim that a minimum detection limit of 2 μg/g should be possible (Jones *et al.*, 1987).

L-XRF vs K-XRF

The most crucial practical differences between L-XRF and K-XRF lie potentially in three areas. One is that use of a Pb/Ca ratio for calibration in K-XRF renders the measurement largely insensitive to geometry and attenuation changes induced by anatomical variation (Somervaille *et al.*, 1985). Thus, unlike with L-XRF, interpretation of a K-XRF measurement is independent of the orientation of the source-detector assembly to the target, and of the target bones within surrounding soft tissue. Bones at various sites can be measured without having to restandardize the measurement for geometry. In addition, adjustment of the measurement for overlying skin thickness (which introduces another level of potential measurement error) is not necessary.

A second potential difference concerns the radiation dose involved in the respective measurements. L-XRF uses poorly penetrating X-rays; thus there is a large drop-off in radiation dose from the skin to the bone marrow, unlike with K-XRF. Direct comparison of radiation risk conferred by the two techniques is complicated by a paucity of experimental data obtained at similar levels of sensitivity. For the purpose of this review, we have assumed a model of the lower limb and used skin doses published in the literature and from our own work. Since the patient of greatest concern is the young child, the lower limb model has been appropriately scaled. The overlying tissue thickness has been taken as 4 mm thick with a density of 1 g/cm^3. The cortical (tibial midshaft) bone thickness has been given a value of 4 mm with a density of 1.25 g/cm^3, and the active marrow diameter has been given a value of 5 mm with a density of 1 g/cm^3.

Measures of skin exposure and estimates of bone marrow exposure and absorbed organ equivalent dose comparing L- and K-XRF systems are supplied in Table 1. The L-XRF system data are described by Wielopolski *et al.* (Wielopolski *et al.*, in press). The K-XRF system data are from our own work. They result in conservative estimates, given that exposures and doses for K-XRF published by other authors have been the same or lower (Somervaille *et al.*, 1988; Jones *et al.*, 1987). A full description of assumptions and steps in the calculations is given in the Appendix. The absorbed organ equivalent dose for L-XRF is estimated at 0.29 mrem (2.9 μSv) for an extrapolated sensitivity of 6.4 μg/g, whereas the absorbed organ equivalent dose for K-XRF is estimated at from 0.40 mrem (4.0 μSv) for an extrapolated sensitivity of 5 μg/g.

The excess mortality risk including up to 25 years from the time of exposure from a bone marrow radiation dose of 1 Sv has been estimated at 20×10^{-4} deaths (ICRP, 1982). The organ equivalent dose for an intraoral dental X-ray is typically 10 μSv, and is 300–900 μSv for a chest X-ray (ICRP, 1982). Thus, although the K and L techniques involve different energies, the radiation risks are similar to each other and low compared to other standard radiologic techniques. Bone sites that have been chosen so far are also far from any other critical organs.

A third potential difference is that the distinct levels of energy in K-XRF versus L-XRF results in a difference in the type of bone contributing to the lead measurement. The incoming beam and the fluorescence of K-X-rays are typically between 75 and 88 keV in energy. The half-value thickness (the thickness at which the beam is attenuated to one-half) for 80 keV in bone is 2 cm and in soft tissue is

TABLE 1
COMPARISON OF L AND K X-RAY EXPOSURE RISKS[a]

Technique	Mean photon energy (keV)	Skin exposure mrad (mGy)	Skin area exposed (cm^2)	Exposure at bone marrow mrad (mGy)	Volume of marrow exposed (cm^3)	Absorbed organ equivalent dose[b] mrem (μSv)
L-XRF	20	1040 (10.4)	5	198 (1.98)	0.5	0.29 (2.9)
K-XRF	88	325 (3.25)	2.0	273 (2.73)	0.5	0.40 (4.0)

[a] Using data from our own KXRF system.
[b] Assuming 0.334 kg of red marrow in an 18-kg child.

4 cm. This means that K-XRF will sample deeply and relatively uniformly into a bone site several centimeters thick. The half-value thickness of the low energy L-X-rays, however, is on the order of 0.5 mm. The fact that lead content in the outer 0.5 mm of bone contributes most of the measurement in L-XRF may have important implications given the possibility that lead kinetics in this subperiosteal layer of bone may be quite different than deeper cortical bone (see subsequent discussion).

The Distribution of Lead in Bone

Although XRF may successfully measure lead content in bone, it is unclear what significance should be attached to that measurement. While a full understanding may await epidemiologic studies, a review of available knowledge on the distribution of lead in bone is warranted to anticipate what that significance may be and to guide in the selection of technique and bone(s) being examined.

A number of investigators have collected data consisting of atomic absorption analyses of bone specimens in populations. Comparisons between studies is complicated by differences in units, with studies varying between describing bone lead content as micrograms of lead per gram wet bone, per gram dried bone, or per gram ashed bone. In this paper, lead content will be discussed in terms of micrograms lead per gram ashed bone unless otherwise stated.

Cortical vs Trabecular Bone

Much research has consisted of comparisons of bone lead content from a few selected sites in individuals exposed to lead in the general environment. From these studies, it was noted that dense bones that are composed mostly of cortical bone generally had higher lead concentrations (mcg of lead per gm wet or dry bone) than lighter bones that are composed mostly of trabecular bone, and that both types of bone had lead contents that were far higher than any soft tissue organ (Barry and Mossman, 1970; Barry, 1975; Horiuchi *et al.*, 1959; Schroeder and Tipton, 1968; Strehlow and Kneip, 1969).

It has also been noted that the ratio of trabecular to cortical bone lead content changes with age, belying differences in kinetics. Age-stratified analyses of data on lead in dense (highly cortical) bone show a linear increase in concentration with advancing age (Barry and Mossman, 1970; Barry 1973, 1975; Holtzman *et al.*, 1970), whereas similar analyses of data on lead in spongy (highly trabecular) bone show a linear increase in lead concentration with age until the fifth decade, when concentrations show a leveling off or decrease (Schroeder and Tipton, 1968, Schroeder and Balassa, 1961; Cherry *et al.*, 1974; Nusbaum *et al.*, 1965). Studies in which lead content in both dense and spongy bone were measured in each skeleton (Gross *et al.*, 1975; Wittmers *et al.*, 1988) have also shown a steady increase in lead content in dense bone with age, but a leveling off or decrease in spongy bone lead content in later years (Fig. 3).

Research on trabecular and cortical bone lead content in subjects exposed to much higher lead concentrations have found even more dramatic differences. In studies of lead-exposed workers in which lead concentrations in mostly cortical bone were compared with lead concentrations in mostly trabecular bone among

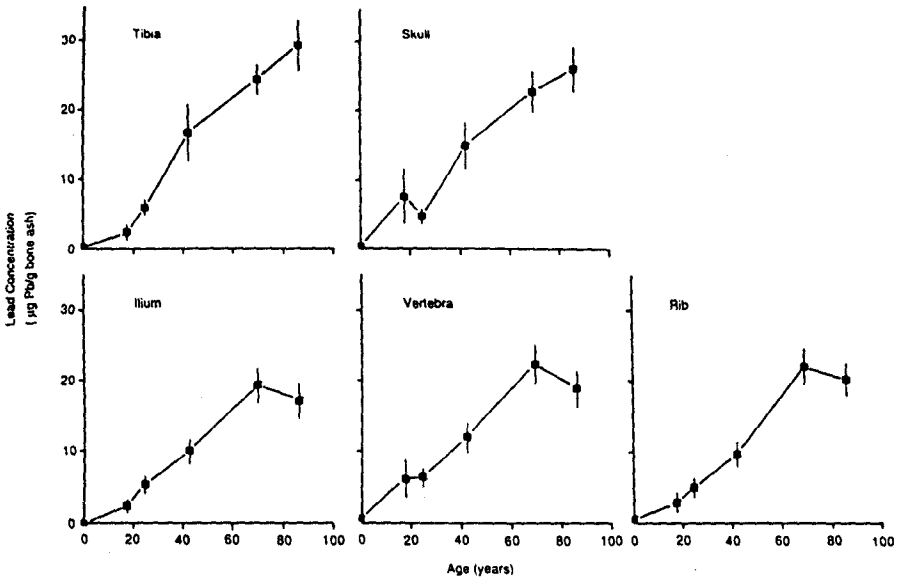

FIG. 3. Bone lead concentration at the five bone sites as a function of age group. (From Wittmers *et al.*, 1988. Reprinted with permission of the Helen Dwight Reid Educational Foundation. Published by Heldref Publications.)

active and retired workers, markedly different ratios were found, suggesting kinetic differences in the handling of lead (Skerfving *et al.*, 1983; Christofferson *et al.*, 1986, 1987; Somervaille *et al.*, 1986).

The difference in lead content between trabecular and cortical bone seen in these studies is not surprising. Research on the biodynamics of bone as well as specific experimental observations on the behavior of lead in bone provide a theoretical basis for differentiating the kinetics of the two bone types with respect to lead. Two major processes seem to be responsible.

Some, if not most, lead ions that infiltrate into bone have been observed in X-ray diffraction studies to become incorporated into the crystalline structure of the bone salt, much like other "bone volume seekers" such as strontium and radium (MacDonald *et al.*, 1951). Accordingly, the amount of lead exchange between bone and surrounding tissue fluid would be expected to depend to a high degree on bone turnover rate (Jaworski, 1965; Smith and Hursh, 1977). General metabolic turnover rates between the two bone types, as measured by isotope studies, have long been known to differ (Rivera, 1965; Rabinowitz *et al.*, 1973, 1976). This may be a function of the ratio between bone surface exposed to remodeling activity and mass, the ratio being two to 40 times greater in trabecular bone than cortical bone (Frost, 1973).

As calculated for the ^{90}Sr fractional transfer rates from bone, trabecular bone has been estimated to have a turnover half-time of 2.4 years, whereas the half-time for cortical bone is estimated at 9.5 years (Papworth and Vennart, 1984). Studies of bone mass with respect to age demonstrate clear difference in rates of decline

between trabecular and cortical bone, particularly in postmenopausal females (Mazess, 1982), suggesting accelerated resorption in trabecular bone that is likely accompanied by increased overall turnover.

It has also been suggested that some lead ions enter and exit bone volume by diffusion without becoming "permanently" incorporated into bone crystal lattice (Marcus, 1985; Marshall and Onkelinx, 1968). Under this model, an important factor governing the rate of ionic lead transfer would be the exchange of lead at the interface between bone and surrounding tissue fluids and blood. The surfaces involved would chiefly include those constituting the walls of the lacunae, of the canaliculi, and of the Haversian and Volkmann's canals (Smith and Hursh, 1977). Since total skeletal trabecular bone has been estimated to have a surface area that is equivalent to cortical bone (Lloyd and Hodges, 1971), despite accounting for only 20 to 30% of total bone mass (ICRP, 1975; Frost, 1963), one could expect trabecular bone to allow a greater amount of ingress and egress of lead ions irrespective of architectural bone turnover.

Several authors have utilized available data to develop multicompartmental models, with separate trabecular and cortical bone lead compartments, that predict lead concentrations under varying conditions (Bernard, 1977; Chamberlain, 1985; Marcus, 1985; Christoffersson *et al.*, 1987). The half-lives found vary widely, with the half-life of cortical bone lead calculated to be just a few years in some studies, to over 50 years in others. Lack of agreement may reflect the difference between basing calculations on data from populations exposed to low lead levels versus occupationally exposed subjects with high lead levels (Christoffersson *et al.*, 1987).

Since transfer of lead ions is bidirectional, one would expect that trabecular bone will not only lose lead content more quickly over time, as seen in general populations exposed to low levels of lead, but will also absorb lead more quickly given elevated exposure levels. Trabecular bone lead concentrations should be greater than those of cortical bone in some individuals with current occupational exposure to lead. This has been observed in some studies (Skerfving *et al.*, 1983; Somervaille *et al.*, 1986).

With respect to the application of XRF, a bicompartmental model of lead kinetics in bone has two important implications: (1) A single summary estimate of skeletal lead content may be less informative than separate estimates of trabecular and cortical bone. Separate estimates should ideally be made for each compartment in epidemiologic studies, since lead content in each compartment may have distinct ramifications for toxicity. (2) If, nevertheless, one wanted to derive an accurate assessment of total skeletal lead content, it would be necessary to extrapolate using separate measurements of lead content in trabecular and cortical bone, as well as an estimate of the proportion of cortical to trabecular bone for the entire skeleton. This fraction has been given an approximate value by some authors (ICRP, 1975), but is probably quite variable and partially dependent on age.

Homogeneity within Bone Type

Other than the measurement error and limit of detection of the instrument itself, a major factor that will determine the precision of an XRF measurement is the

biological variation of lead distribution within the compartment being measured, whether it be trabecular or cortical bone. Scant data, however, are available in the literature with which to assess this issue, since few studies measured lead content in multiple bone sites; and among those that did, few analyzed their data from this perspective.

It can be seen from some studies that the mean concentrations of lead content in bones that were composed mostly of the same bone type, such as tibia and skull, or vertebra and rib, were roughly the same (Barry and Mossman, 1970; Barry, 1975; Gross *et al.*, 1975), inasmuch as the mean concentrations were different between the two bone types.

Specific analysis of intracompartment variation is available from few studies. In one recent autopsy study, 3-mm-diameter samples were extracted from multiple bone sites in 134 cadavers using a drill-driven hollow core bit (Wittmers *et al.*, 1988). The bones examined included the midshaft tibia and occipital bone, two predominantly cortical bones, and vertebra, iliac crest, and rib, three predominantly trabecular bones. In addition, multiple samples were taken from several vertebrae to assess trabecular bone homogeneity: from the length of a single tibial diaphysis to asses intrabone homogeneity, and from left and right bones of a separate series of 12 human skeletons to assess lateral homogeneity.

Interbone intracompartment homogeneity of lead content was assessed by comparing linear regression correlations of bone site pairs. When bones of mostly cortical architecture (skull and tibia) were matched with each other, and bones of mostly trabecular architecture (vertebra, ilium, and rib) were matched with each other, resultant correlations showed significantly better agreement in all age categories. This is in contrast to intercompartment (vertebra/tibia) correlation analysis (Table 2) and suggests that cortical bone lead concentration, indeed, is distinct from trabecular bone lead concentration in all bones.

Comparison of lead concentrations between right and left tibias of the separate series of 12 skeletons provided data with which to assess intrabone intracompartment homogeneity of lead content (Wittmers *et al.*, 1988). This revealed lateral symmetry throughout a range of lead levels (Fig. 4), with a calculated correlation coefficient of 0.98.

TABLE 2
LINEAR REGRESSION CORRELATION[a] OF BONE SITES AS A FUNCTION OF AGE

Age group	14–20	21–35	36–50	57–75	>75
Data pairs[b]					
S/T[c]	1.247 (.97)	0.947 (.82)	0.919 (.95)	0.989 (.93)	0.815 (.88)
V/R[c]	1.071 (.95)	1.093 (.92)	1.144 (.72)	0.941 (.76)	0.893 (.74)
V/T[c]	1.315 (.94)	1.112 (.62)	0.837 (.76)	0.906 (.64)	0.557 (.52)

[a] Correlation was accomplished with the equation $y = mx$; that is, the intercept was forced through (0, 0).

[b] The number in parentheses represents the correlation coefficient (R) for each of the sample site pairs.

[c] Adapted from Wittmers *et al.*, 1988. S, skull; T, tibia; V, vertebra; R, rib.

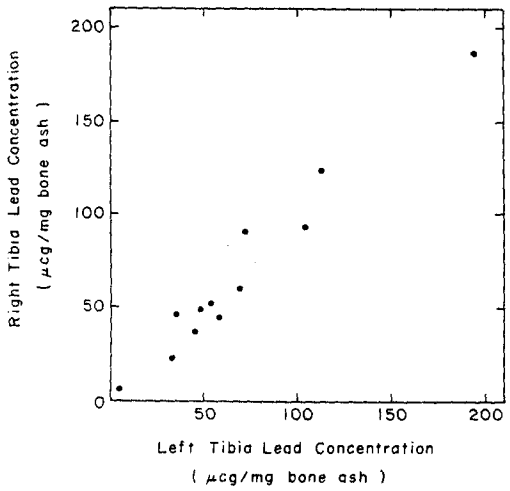

FIG. 4. Right and left tibia bone lead concentrations in 12 skeletons. (Adapted from Wittmers *et al.*, 1988. Reprinted with permission of the Helen Dwight Reid Educational Foundation. Published by Heldref Publications.)

However, in another test of intrabone homogeneity, the variation in lead content was examined in 28 core samples of 3-mm width obtained along the mostly cortical bone shaft of a single tibia. Values ranged from 21 to 37 mcg/mg bone ash, with a mean of 28.5 μcg Pb/g and standard deviation of 4.1 μcg Pb/g ash.

Since the coefficient of variation of the lead analysis employed has been measured at 9 to 12% (Wittmers *et al.*, 1981), the variation in lead content seen in these core samples probably represents true biological variation in lead distribution within the cortical bone compartment.

This is consistent with a separate series of bone lead analyses conducted in specimens we collected. In this work, 1-cm-thick cross-sectional slices were obtained at various locations on the tibia, patella, and calcaneus of two amputation specimens. Slices were divided into quadrants, and then cortical bone was carefully separated from trabecular bone. After weighing and ashing, samples were then analyzed by graphite furnace atomic absorption spectrometry (Wittmers *et al.*, 1981).

Quadrant specific data (Table 3) show a variation in lead content within some slices of a considerable degree, both in cortical and trabecular bone. A possible explanation for this intracompartmental variation is that, on the relatively small scale afforded by 3-mm core samples and 1-cm cross-sectional bone wedges, there is potentially a large amount of variation in the number of active osteons that would be avidly depositing lead. For instance, the retention of radium in the adult skeleton is quite nonhomogenous on the scale of a cross-sectional slice, as seen in the autoradiograph of a tibial cross-section from a patient with radium poisoning who was given ^{226}Ra therapeutically for 1 year at the age of 46 years, and who died 36 years later (Fig. 5).

Lead concentrations in larger bone samples would no doubt give more stability

TABLE 3
LEAD CONCENTRATION (μcg/g BONE ASH)

Bone site (mean (SD))	Quadrant 1	2	3	4	
	Amputation specimen 1				
Tibia mid-diaphysis C:	50.1	44.3	52.8	40.1	46.8 (5.7)
T:	53.7	55.6	56.3	68.3	58.5 (6.6)
Calcaneus C:	60.0	67.7	70.3	85.1	70.8 (10.5)
T:	38.5	49.9	50.9	54.7	48.5 (7.0)
	Amputation specimen 2				
Tibia mid-diaphysis C:	51.9	58.2	62.7	64.1	59.2 (5.5)
T:	59.5	32.2	61.2	69.7	55.7 (16.3)
Tibia proximal metaphysis C:	58.9	48.1	87.2	61.4	63.7 (16.7)
T:	29.2	30.5	50.9	33.0	35.9 (10.1)
Patella C:	71.6	56.7	67.1	52.8	62.2 (8.8)
T:	55.8	57.9	51.8	45.7	52.8 (5.4)
Calcaneus C:	62.2	97.6	35.8	21.9	54.4 (33.3)
T:	29.2	35.8	23.6	23.6	28.1 (5.8)

Note. C, cortical bone; T, trabecular bone.

to intracompartment lead estimates. This confers an advantage to XRF, which is likely to use a field width of several centimeters of bone to derive measurements. Should lead content on the level of the osteon be proved to vary as suggested, large bone analysis with XRF may also be more appropriate than atomic absorption of small bone samples as a method of mapping skeletal lead distribution in future studies.

In addition to variability between quadrants, however, the data in Table 3 suggest interbone intracompartment differences in lead content, particularly in trabecular bone. Calcaneal trabecular bone shows consistently lower lead content than the tibia and patella, raising the issue of whether a bicompartmental model glosses over significant bone site differences in lead kinetics. Indeed, turnover rates in the movement of calcium and other alkaline earths have been shown to be quite different in different bones (Vaughan, 1981).

Surface Bone

An additional aspect of skeletal lead distribution that is relevant to XRF concerns the characteristics of surface bone (bone closest to the periosteum). The L-XRF technique uses energy of low penetrating power. A consequence is that over 75% of its measurement is derived from the outer 0.5 mm of bone in the path of the beam.

Authors using L-XRF have assumed that the technique estimates cortical bone lead content on the gross appearance of bone architecture that shows cortical bone as the peripheral supporting structure of most bone. A problem with this assumption, however, is that it does not take into account the biodynamics of bone.

Several histomorphometric studies in humans have shown that periosteum

FIG. 5. A no-screen autoradiograph of a complete tibia cross section from a case of radium poisoning (Case 118) given radium therapeutically for 1 year at age 46 years, estimated body burden 10 μcg at death 36 years later. Note random pattern of hot spots. (From Rowland and Marshall, 1959. Reprinted with permission from the publisher.)

probably remains active, forming new bone, throughout adulthood (Epker *et al.*, 1965; Epker and Frost, 1966). This is reflected by the increase in total cross-sectional area that is seen throughout life in several bones, including the femur, tibia, and ribs (Epker, 1974; Ruff and Hayes, 1982). The addition of new bone on the peripheral surface is counterbalanced by the resorption of bone from within (on the endosteal surface), a process which is ultimately responsible for the total decrease in bone mass which is seen with aging (despite the continual new addition of bone at the periosteal surface).

New bone is felt to allow greater diffusion of bone-seeking elements, due to its low mineral density-high permeability nature (Frost, 1963). Thus, with respect to lead kinetics, surface bone under the periosteum may actually behave less like cortical bone and more like trabecular bone, despite having a cortical bone architecture.

Evidence in support of this view can be found in a recent study in which a cross-section of femur from a lead-exposed worker was analyzed for lead content with proton induced X-ray emission (Lindh *et al.*, 1978). Using a microprobe technique, the investigators created a map of lead distribution within the bone cross-section that demonstrated uneven peaks (Fig. 6). It can be clearly seen that

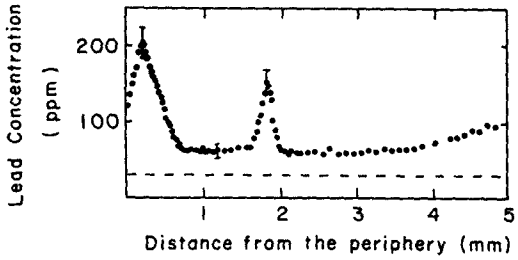

FIG. 6. Concentrations of lead as a function of distance from the periphery of femur bone. (From Lindh *et al.*, 1978. Reprinted with permission from the publisher and authors.)

the outer 0.5 mm of cortical bone is associated with a lead concentration peak that is over two times the level of the rest of the cortex. The separate, inner peak beginning at 1.7 mm from the surface may represent elevated lead absorption by subperiosteal bone a number of years earlier, when the femur was of a smaller diameter. Preliminary results from experiments using the PIXE technique on a slice of tibial diaphysis at Brookhaven National Laboratory also reveal a pattern of lead peaking in the outer 1 mm of subperiosteal surface bone compared to inner cortical bone (Jones, 1988).

It is possible that surface bone lead content has important toxicologic significance of its own. Preliminary work has been published demonstrating than an elevated lead level as detected by L-XRF is highly specific (although poorly sensitive) for an elevated response to EDTA mobilization tests in children (Rosen *et al.*, 1987). Not enough is known to prioritize the biological significance of surface, cortical, and trabecular bone lead contents.

Deciding Which Bones to Measure with XRF

K-XRF measures the concentration of lead throughout the thickness of bone being examined. In order to obtain pure estimates of lead content in trabecular and cortical bone, an obvious approach would be to examine bone or bone segments that were composed entirely of trabecular bone separately from areas that were composed entirely of cortical bone. No bone attains 100% purity of composition; however, several bones have segments that approach 90–95% purity of trabecular or cortical bone type. For example, the middiaphyseal portions of the long bones, range from 85 to 99% cortical bone; the vertebrae, in contrast, are approximately 90% trabecular composition.

Additional considerations are to select bone sites that are (1) easily accessible to the XRF tool, (2) can be standardized from individual to individual, (3) minimize risk from radiation by avoiding radiosensitive organs, and (4) afford large bone volume, in order to maximize the lead signal. These considerations lead to a focus on large bone sites in the peripheral appendicular skeleton.

Midshaft tibia has emerged as a site frequently used for XRF measurements. It is composed of 95% cortical bone, is easily located anatomically, and affords substantial bone volume for the measurement.

There has been little experience, however, in selecting a site for XRF measurements that is primarily trabecular bone.

The recent surge of interest in osteoporosis and bone fractures has prompted cross-sectional bone mapping studies that yield helpful data. In a study by Ruff of 20 tibiae from adults aged 30 to 90, cortical and trabecular bone areas were measured from cross-sectional slices of bone at various intervals (Ruff, 1988). A previously developed technique was used in which bones were embedded in rigid foam and sectioned transversely at various points along the tibia (Ruff and Hayes, 1988). Photographs of each section surface with a superimposed grid were then rear-projected onto a digitizer screen and manually traced according to architecture. In Table 4 and Fig. 7, it can be seen that the proximal metaphysis is primarily trabecular bone in cross-sectional area (and volume). Using an estimate of proximal metaphyseal cortical bone density of 1.90 g/cm^3 (Ruff and Hayes, 1984), and of proximal metaphyseal trabecular bone of 0.31 g/cm^3 (Carter and Hayes, 1977), the proximal metaphysis by weight is still primarily trabecular bone.

Two other lower extremity bone sites may be suitable for trabecular XRF measurements (Fig. 8). Somervaille *et al.* have explored the utility of the calcaneus as a primarily trabecular bone for XRF measurements (Somervaille *et al.*, 1987). It is a prominent, easily accessible bone for *in vivo* measurements, and in a study of amputations specimens comparing XRF of the calcaneus with atomic absorption spectrometry of calcaneal biopsy specimens, a good correlation was found.

Similarly, the patella is prominent and generally believed to be composed primarily of trabecular bone. However, no quantitative data exist for either bone regarding exact trabecular/cortical bone composition in the general population. In addition, the variability seen in trabecular bone lead content at these sites (Table 3) makes it unclear which bone site may be most representative of overall trabecular bone lead content.

SUMMARY

XRF promises to provide a noninvasive, rapid, relatively accurate and precise measurement of lead content in bone. The choice between using an L-XRF or K-XRF instrument may depend on issues of cost, technical considerations of sensitivity, and on whether information sought on bone lead content is best supplied by

TABLE 4
TWENTY TIBIA SPECIMENS (AGE RANGE 32–99, 10 MALES, 10 FEMALES)

Slice	Distance of slice from proximal tibia plateau, expressed as % of tibial length	Cortical area (mm^2 (SD))	Cortical mass[a] (g/mm^3)	Trabecular area (mm^2 (SD))	Trabecular mass[b] (g/mm^3)	% Trabec by surface area/volume	% Trabec by mass
A	2	154 (6.0)	293	2794 (160.9)	866	95	75
B	5	142 (6.3)	270	2551 (139.2)	791	95	75
C	10	162 (16.3)	308	1191 (82.9)	369	88	55
D	50	251 (15.7)	477	<10	<3	<5.0	<1.0

[a] Assuming a slice thickness of 1 mm and a cortical bone density of 1.90 g/cm^3.
[b] Assuming a slice thickness of 1 mm and a trabecular bone density of 0.31 g/cm^3.

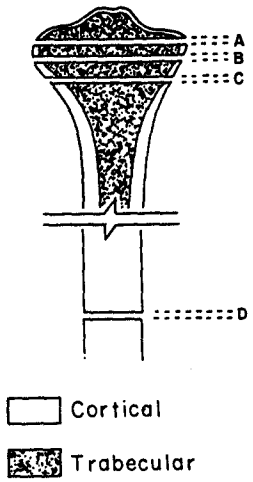

FIG. 7. Cortical and trabecular bone surface area in cross-sectional slices of the tibia.

a subperiosteal surface bone (L-XRF) measurement, or full-thickness bone measurement (K-XRF) of one or several bones, or both. Due to the distinct kinetics of lead in trabecular and cortical bone, investigations on the toxic effects of bone lead stores would be benefited by separate estimates of trabecular and cortical

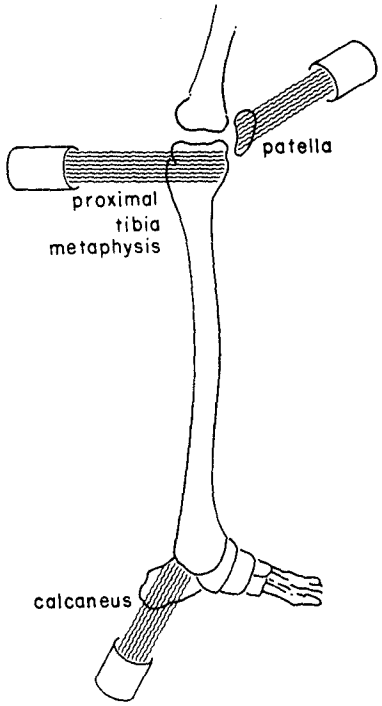

FIG. 8. Possible sites for XRF measurement of trabecular bone.

bone lead stores. The tibia has emerged as a useful site for K-XRF measurements of cortical bone lead stores. Candidates for K-XRF measurements of trabecular bone include the proximal metaphysis of the tibia, calcaneus, and patella, and perhaps others.

Research is needed in several areas to further define the use of XRF. Skeletal research is needed to assess the uniformity of lead distribution in trabecular bone, and the ratio of cortical to trabecular bone, particularly at bone sites being contemplated for K-XRF measurement. Bone studies in animals or humans with known lead-exposure histories would facilitate the interpretation of cortical and trabecular XRF measurements. More intrabone mapping studies using proton induced X-ray emission (PIXE) should be performed in order to assess the issue of whether subperiosteal surface bone has lead kinetics that are distinct from cortical and trabecular bone. If they are distinct, studies using both K-XRF and L-XRF may be needed to compare the full toxicologic significance of lead measurements derived from each technique.

As the XRF technique is honed, the scope of its potential application is, indeed, wide. Skeletal lead burden would be an invaluable exposure variable in epidemiologic studies on the relationship of lead exposure to blood pressure, kidney disease, cognitive development, fertility, and other outcomes. It would also provide a useful method for assessing body burden in clinical settings, such as in the work-up of children suspected of having lead toxicity, the monitoring of workers in lead-exposed occupations, or the assessment of treatment results and needs in patients undergoing lead chelation.

APPENDIX

Methods Used in Exposure Risk Calculation in Table 1

Mean Photon Energy

For the L-XRF, Wielopolski *et al.* obtained the mean photon energy of their X-ray generator by deconvolution of the scattered photon spectrum and verified the calculation by half-value layer measurements in aluminum. For K-XRF, there is one γ-ray incident.

Skin Dose

These are quantities measured by either thermoluminescence detectors, film badges, or calibrated rate meters.

Skin Area Exposed

Measured or straightforward geometry calculation.

Dose at Bone Marrow

The skin dose was multiplied by the coefficient describing attenuation through the skin and bone layers. The model used a 4-mm skin thickness with a density of 1 g/cm^3, a 4-mm bone thickness with a density of 1.25 g/cm^3, and mass attenuation coefficients according to the following table taken from the U.S. Public Health Service Radiological Health Handbook (U.S. PHS, 1970).

Photon energy (key)	Skin attenuation coefficient (cm^2/g)	Bone attenuation coefficient (cm^2/g)
20	0.793	2.79
88	0.177	0.195

Volume of Marrow Exposed

Calculated on the basis of beam spot geometry and an assumed marrow cavity of 5 mm in diameter. Volume = cavity cross section × length of cavity exposed. This column is an approximation, as it does not take into account scattering and secondary radiation generation. However, it is adequately correct for comparison purposes.

Organ Equivalent Dose

Dose = dose at bone marrow × quality factor × volume marrow exposed × density of marrow/total body red marrow mass. For this calculation, density of the marrow was assumed to be 1 g/cm^3. The total red marrow mass was obtained by scaling the "standard man" of 70 kg with 1.3 kg red marrow to an 18-kg child (U.S. PHS, 1970). The quality factor for X- or γ-rays is 1.

ACKNOWLEDGMENTS

This work was supported by National Institute for Environmental Health Sciences Environmental Training Grant ST 32 ES 07069 and National Institutes of Health/Small Business Innovation and Research Grant 2R44 ES03918-02. Thanks are due to Dr. A. C. Aufderheide and Ms. JoAnn Wallgren for atomic absorption spectroscopy analysis of bone specimens described in Table 2 and to Dr. C. Ruff for bone slice data described in Table 3. Drs. Tor Tosteson, Frank Speizer, and Scott T. Weiss provided helpful comments on the manuscript.

REFERENCES

Ahlgren, L., Lidén, K., Mattsson, S., and Tejning, S. (1976). X-ray fluorescence analysis of lead in human skeleton *in vivo*. *Scand. J. Work Environ. Health* 2, 82–86.

Ahlgren, L., Haeger-Aronsen, B., Mattsson, S., and Schütz, A. (1980). In-vivo determination of lead in the skeleton after occupational exposure to lead. *Brit. J. Ind. Med.* 37, 109–113.

Araki, S., Murata, K., and Aono, H. (1986). Subclinical cervico-spino-bulbar effects of lead: A study of short-latency somatosensory evoked potentials in workers exposed to lead, zinc, and copper. *Amer. J. Ind. Med.* 10, 163–175.

Araki, S., and Ushio, K. (1982). Assessment of the body burden of chelatable lead: A model and its application to lead workers. *Brit. J. Ind. Med.* 39, 157–160.

Aub, J. C., Robb, G. O., and Rossmeisl, E. (1932). Significance of bone trabeculae in the treatment of lead poisoning. Lead studies XVIII. *J. Public Health* 22, 825–830.

Barker, D. J. P., Chamberlain, A. T., Detheridge, F. M., Gardner, M. J., and Guyer, P. B. (1982). Low lead levels in Pagetoid bone. *Metab. Bone Dis. Rel. Res.* 4, 243–247.

Barry, P. S. I. (1973). A comparison of lead concentrations in human bones and in soft tissues. *In* "Environmental Health Aspects of Lead, International Symposium" (Commission of the European Communities and the United States Environmental Protection Agency), pp. 415–426. Directorate General for Dissemination of Knowledge, Commission of the European Communities, Luxenbourg.

Barry, P. S. I. (1975). A comparison of concentrations of lead in human tissues. *Brit. J. Ind. Med.* 32, 119–139.

Barry, P. S. I., and Mossman, D. B. (1970). Lead concentrations in human tissues. *Brit. J. Ind. Med.* 27, 339–351.